Astronomical Data Analysis Software and Systems XV
ASP Conference Series, Vol. 351, 2006
C. Gabriel, C. Arviset, D. Ponz and E. Solano, eds.

Wavelet-Based Image Deconvolution for Wide Field CCD Imagery

Maria Teresa Merino[1], Octavi Fors[12], Xavier Otazu[3], Rob Cardinal[4], Jorge Núñez[12], A.R. Hildebrand[4]

Abstract. We show how a wavelet-based image adaptive deconvolution algorithm can provide significant improvements in the analysis of wide-field CCD images. To illustrate it, we apply our deconvolution protocol to a set of images from a Baker-Nunn telescope. This f/1 instrument has an outstanding field of view of 4.4°x4.4° with high optical quality offering unique properties to study our deconvolution process and results. In particular, we obtain an estimated gain in limiting magnitude of $\Delta R{\sim}0.6$ mag and in limiting resolution of $\Delta\rho{\sim}3.9''$. These results increase the number of targets and the efficiency of the underlying scientific project.

1. Introduction

Signal processing has progressed significantly during the last decade. The development of the multiresolution concept based on wavelets and the use of adaptive deconvolution by using signal detection masks have improved the performance of traditional algorithms, specially in terms of noise amplification reduction, a crucial aspect in astronomical images (Starck et al. 2002).

But deconvolution in Astronomy is still usually restricted to a few particular applications where the original images have some specific ideal properties. In undersampled or poorly sampled images, it is known that deconvolved images usually violate the sampling theorem (Magain 1998) introducing problems in the posterior analysis such as accurate astrometry and photometry. Moreover, in cases such as wide field instruments' data with noticeable distortions we also face additional complications such as variable background and variable PSF across the image, problems obtaining acceptable flats, etc.

The aim of this example is to show how a wavelet-based Bayesian adaptive deconvolution algorithm can also provide important improvements to those projects with data showing non-ideal features. In the following sections we describe the techniques used, the data processed and how deconvolution can make significant improvements to achieve the underlying scientific goals.

[1]Departament d'Astronomia i Meteorologia, Universitat de Barcelona, Spain

[2]Observatori Fabra, Barcelona, Spain

[3]Centre de Visió per Computador, Universitat Autònoma de Barcelona, Spain

[4]Rothney Astrophysical Observatory, University of Calgary, Canada

2. Baker-Nunn Data Deconvolution

We deconvolved ten, 30s, 0.8°x0.8° central subframes of the same region of the sky obtained in a not ideal night (seeing$\sim 3''$) with FWHM$\sim$2.1 pixels using the Baker-Nunn Telescope at the Rothney Astrophysical Observatory (Calgary).

Baker-Nunn cameras were built during Cold War as 50cm f/1 photographic modified Schmidt altazimutal instruments for satellite tracking. Rothney's was retrofitted to work with a 4kx4k-9μm CCD providing a field of view of 4.4°x4.4° with high optical quality (spot size $\sim$ 20μm) and $3.9''$/pixel. It is searching for NEOs in the North pole regions since 2003 (NESS-T project), though some calibrations are still being held to evaluate other possible uses as variable stars studies. Some of us are retrofitting another Baker-Nunn in Spain (Núñez et al. 2003) with some differences in optical design and observational strategy. These instruments show unique properties and allow very fast and efficient surveys.

To increase NEOs detections it is crucial to push limiting magnitude as faint as possible. Besides, its sampling (close to be critical) results in common object blending, so it is also important to improve the deblending and resolution of the detected objects. These are the main goals of deconvolving this wide field marginally sampled data even though it has some additional properties not desired for this kind of processing (variable background and PSF, difficulties in obtaining proper flats, overblooming, ...).

The deconvolution algorithm used is a modified MLE (Gauss+Poisson) using wavelets and adaptive deconvolution. The basic primitive algorithm belongs to the group based on a maximum likelihood estimator (MLE) derived through Bayesian methodology considering noise being Poisson and Gauss. Our implementation, named AWMLE, was upgraded (Otazu 2001) to incorporate the multiresolution concept working onto wavelets decomposition and the adaptive deconvolution using probability masks. These additional features allow detection and deconvolution of only real signal features and minimize noise amplification and false detections.

A new methodology for this application was defined (Fors 2006): (1) CCD frames calibration; (2) astrometric plate transformation of every frame I_i to I_1 and then also to the reference catalog USNOA2.0 (Monet et al. 1998); (3) aperture photometry of reference stars and PSF fitting with a subset of best candidate stars with different PSF models hybrid (Gaussian, Moffat15 and Lorentz) and purely analytical (Penny); (4) frames deconvolution with each PSF model keeping partial results up to 200 iterations; (5) object detection with `SExtractor` (Bertin & Arnouts 1996) at 2σ and 3σ thresholds with dark nature effects masked; (6) matchings between all frame-catalogs and matchings with USNOA2.0; (7) false detections and deblending analysis at 2σ-threshold; (8) limiting magnitude gain with respect to USNOA2.0 (R-mag) at 3σ-threshold. Most steps were done with `IRAF` (Tody 1986), or with custom processing tools.

3. Results

PSF influence: Moffat15 delivered a larger number of matched detections (maximum at $\sim$140-iter) but Lorentz reached its maximum earlier (at $\sim$120-iter) with significantly less false detections. Differences are from Moffat15 minimal

residuals in the core compared to Lorentz's better fit to the outer wings of the PSF. Gaussian and Penny gave poorer results because are worse fitting models for this data. The non-assymptotic convergence in detections vs. iterations over the maximum is due to not having a well estimated background and flat-field.

Table 1. Original, Moffat15(140-iter) and Lorentz(120-iter) 2σ-detections

Image	Raw	Matched	Unmatched (%)
Original	1734	1724	0.4
Moffat15 (140 iterations)	2733	2644	3.2
Lorentz (120 iterations)	2677	2610	2.5

False Detections: Table 1 shows results for one of the frames and its best deconvolutions. Most of the few unmatched detected objects are due to PSF mismatch and ringing (57 Moffat15, 48 Lorentz), both effects appearing because of the sampling theorem violation, typical in deconvolution of marginally sampled data. Some are false detections because deconvolution of overblooming around bright stars, ghosts created by internal reflections (4 original, 7 Moffat15, 5 Lorenz), or objects not in USNOA2.0 but included in USNOB1.0 (3 original, 4 Moffat15&Lorentz). Only 16 in Moffat15 and 7 in Lorentz remain as true marginal false detections and all them vanished in the 200-iter images. They are very reasonable amounts considering the limited PSF modelling and the non-assymptotic convergence constraints explained above. Moreover, although not being real, we remark the recoveries of the 2 ghosts and the 1 missing object in USNOA2.0 detected in the deconvolved but too faint or blended in the original image. They show that the algorithm could recover some possible slightly faint or blended asteroids. Unfortunately this FOV has no asteroid, but repeating this study with other frames with known faint asteroids is a future work in process.

Resolution Gain: Figure 1a shows near resolved objects vs. separation up to 30 pixels in the original vs. the Moffat15 deconvolved image. Some of the new resolved objects might appear merely because of the increase of new faint detections, but specially for those separations until a few FWHMs most of them are more likely due to the deblending. To compute an estimation of the limiting resolution gain with deconvolution we look at the minimum separation between objects in the original image (3.7 pixels) and in the deconvolved one (2.7 pixels). That leads to a limiting resolution gain of $3.9''$, crucial specially for working in crowded areas with poorly sampled instruments where there is a significant probability of loosing asteroids due to blending with a nearby star.

Magnitude Gain: To evaluate the magnitude gain we do detections with the more usually accepted 3σ threshold instead of the 2σ threshold more common for merely asteroid detection. Matching tolerance radius is 2.25 pixels since showed to be a a good compromise avoiding false matched besides false unmatched due to errors in catalogs, transformations and centroiding. Using USNOA2.0 as reference catalog instead of others more complete or accurate ones is not very relevant for our specific data properties to only get a relative estimate.

Figure 1. a) Resolution Gain b) Magnitude Gain

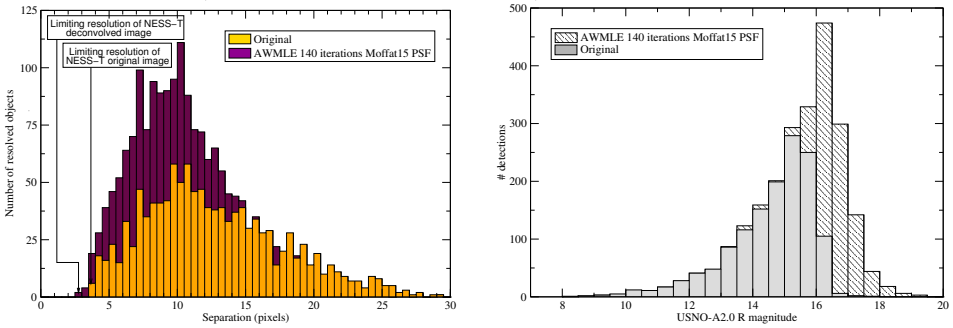

Figure 1b illustrates matched detections vs. USNOA2.0 R-mag for the original and Moffat15(140-iter) deconvolved frames. A dramatic recovery of faint objects by the deconvolution application is shown. The estimate of limiting magnitude gain by simply applying the area ratio of the histograms results in $\Delta R{\sim}0.6$ mag. Note that this ΔR gain estimate does not take into account the intrinsic magnitude distribution in the studied FOV and so could be somewhat biased.

4. Conclusions

Deconvolution can add important benefits to the use of wide field and marginally sampled Baker-Nunn data for NEO surveys, even with difficulties such as the variable PSF and background, not proper flat, overblooming,etc. We show firstly how our deconvolution protocol decisively increases the detections with only a few and reasonable false ones providing a limiting magnitude gain $\Delta R{\sim}0.6$ mag and secondly how improves near objects deblending with limiting resolution gain $\Delta\rho{\sim}3.9''$. Similar improvements by using deconvolution may be also useful to data from other observational facilities usually not considered to be deconvolved.

Acknowledgments. M. Merino is supported by a fellowship from the MEC, Spain, Ref. AP2002-2676; X. Otazu by the program Ramon y Cajal, founded by the MEC; A. Hildebrand by the Canada Research Chair Program.

References

Bertin, E., & Arnouts, S. 1996, A&A, 117, 393

Fors, O. 2006, Dept. Astronomia i Meteorologia, Univ. Barcelona, PhD Thesis

Magain, P., Courbin, F., & Sohy, S. 1998, AJ, 494, 472

Monet, D. et al. 1998, VizieR Online Data Catalog, 1252

Núñez, J. et al. 2003, Proc. Jornadas Científicas 250 Años de Astronomía, 153

Otazu, X. 2001, Dept. Astronomia i Meteorologia, Univ. Barcelona, PhD Thesis

Starck et al. 2002, PASP, 114, 1051

Tody, D. 1986, Proc. SPIE Instrumentation in Astronomy, 627, 733